Bull. Spec. Astrophys. Obs., 2001, 51, 68-80

Evidence for narrow–band oscillations in the optical spectra of the intermediate polars BG Canis Minoris, YY Draconis and GK Persei

N. N. Somov and T. A. Somova

Special Astrophysical Observatory of the Russian AS, Nizhnij Arkhyz 369167, Russia
e–mail: som,tsom@sao.ru

Received November 20, 2000; accepted May 30, 2001.

Abstract. We report the results of dynamic spectroscopy of the intermediate polars (IPs) BG CMi, YY Dra and GK Per obtained at the 6 m telescope with the help of the photon-counting system known as the scanner of BTA. The spectral study of variability of BG CMi and YY Dra revealed Narrow–Band Oscillations (NBOs) or statistically significant features in their power spectra in contrast to GK Per where the oscillations were not found. The NBOs were detected in the spectra of BG CMi at the spin period of the white dwarf (913 s) in the profiles of the Balmer and HeII 4886 Å emission lines. The widths of the features in the power spectra varied from 2–3 Å to 8–10 Å. The power spectra of YY Dra revealed the features at the spin period of the primary and its harmonic. To compare the NBOs in the spectra of different IPs we have counted formally the number of events of detection of the NBOs (NBO-events) in an exposure in the same wavelength range. As a result, the number of the NBO-events in the power spectra of BG CMi is noticeably greater than that of YY Dra and GK Per. It has been found that the number of the NBO-events in the power spectra of the intermediate polars BG CMi, V405 Aur and PQ Gem is about the same. These objects form a group with polar-like magnetic fields (8–20 MG), whereas YY Dra and GK Per are attributed to the objects with weak magnetic fields. This relationship between the strength of the magnetic field of the object and the number of NBO-events in their power spectra is an additional argument in favour of the presence of strong magnetic fields in the regions of formation of the radiation causing the NBO-events in the power spectra of the IPs.

Key words: binaries: close – stars: individual: BG CMi – stars: individual: YY Dra – stars: individual: GK Per – stars: magnetic fields – cataclysmic variables

1. Introduction

Cataclysmic variables (CVs) are the close binary stars in which a Roche lobe–filling late–type secondary transfers matter to a white dwarf primary. Magnetic CVs are the systems with sufficiently magnetized white dwarfs which form two subclasses. Polars or AM Her stars include synchronous systems in which the spin period of the white dwarf is equal or close to the orbital period (Cropper, 1990). Intermediate polars (IPs) or DQ Her stars (Patterson, 1994) contain rapidly and asynchronously rotating white dwarfs. One of the principal criteria for membership in this class (IPs) of stars is the presence of a rapid, highly coherent periodicity in the light curve, usually at the optical or X–ray wavelengths. In addition to this periodicity some intermediate polars manifest emission–line profile variations over the spin period (Patterson, 1994; Penning, 1985; Helier et al., 1987, 1990, 1991; Buckley and Tuohy, 1989, 1990). Spectral observations revealed variations over the spin period or its harmonic of the ratios V/R, radial velocities or equivalent widths of emission lines. Our optical spectral and spectropolarimetric observations (with the circular and linear polarization analyzers) of PQ Gem (RE 0751+14) (Somov et al., 1997, 1998a, 1998b) and V405 Aur (RXJ0558.0+5353) (Somov et al., 2000a, 2000b) detected monochromatic quasi–periodic oscillations or statistically significant features in the power spectra in narrow wavelength passbands (2–3 Å).

NBOs as phenomena were detected not only in the optical spectra of IPs, pulsations (amplitude $\approx$ 15%) within a narrow (0.25 Å) segment of the broad 1242.8 Å N v component in the ultraviolet spectrum of the Her X–1 system were found too (Boroson et

al., 1996).

The purpose of our paper is to search for the NBOs in the spectra of other IPs and to find relationship between presence of the NBOs in the spectra and physical characteristics of the objects. Here we report the results of a study of the NBOs in the optical spectra of BG CMi, YY Dra and GK Per. A short observational history of the objects follows.

2. Observational history

2.1. BG Canis Minoris

BG CMi, as an optical counterpart of the hard X-ray source 3A 0729+103, is a 15th-magnitude blue star with strictly periodic, 913 s and 3.23 hr, optical and X-ray variations (McHardy et al., 1984, 1987). The orbital and spin ephemeris as well as the spin-up rate of the white dwarf were derived from the optical photometry (Augusteijn et al., 1991). The results of a 10 yr photometric program for BG CMi showed a strictly coherent 913 s wave in its light curve (Patterson and Thomas, 1993). The detection of circular polarization in the optical and infrared observations was the strongest argument in favour of the presence of a strong magnetic field (Penning et al., 1986; West et al., 1987). The results of the Ginga X-ray observation revealed the presence of a 847 s modulation in addition to the known orbital and spin periods of 3.25 hr and 913 s (Norton et al., 1992). It was found in spectrophotometric observations that the emission line V/R ratios were variable over the 913 s period (Garlick et al., 1994). Photometric and spectroscopic observations have revealed a strong variability of the dominant light pulsations, rotational (913 s) and orbital (3.23 hr), on a timescale of years. Variations in amplitude of the spin pulsation with epoch generally appear to be anti-correlated with those of the orbital modulation with the former decreasing, while the latter increases. Neither stable periodic signals at other frequencies nor indication of periodicity at the 847 s X-ray period have been found (de Martino et al., 1995).

2.2. YY Draconis

A 16th magnitude cataclysmic variable, presumably a dwarf nova, was detected as an optical counterpart of the hard (2–10 keV) X-ray source 3A 1148+719. The optical and UV spectra of YY Dra are typical of cataclysmic variables, except that the TiO absorption bands of a M dwarf which can be seen at wavelengths longer than 5000 Å. The radial velocities of the emission line Hα indicated a 4.0 hr orbital period, and the IR light curve shows a "double-humped" waveform from the distorted secondary. High-speed photometry in the U band reveals a stable periodicity of about 1% semiamplitude at a period of 275 s, with some power also in the subharmonic at about 550 s (Patterson et al., 1992).

Time-resolved near-infrared (8100–8600 Å) spectrophotometry and Johnson B-band CCD photometry of YY Dra show the presence of the NaI doublet in absorption from the secondary, as well as sharp and broad CaII emission lines. The radial velocity variations of the NaI near-infrared doublet yield an orbital period of 0.164988 ± 0.00023 days. The spectral type of dM4 $\pm$ 1 for the secondary star has been derived. The distance of YY Dra is 155 ± 35 pc (Mateo et al., 1991).

ROSAT observations of YY Dra revealed pulses with a period of 264.6 ± 1.2 s, confirming the presence of a rapidly rotating magnetic white dwarf. Comparison with the periods observed in the ultraviolet and blue light indicates that the 275 s ultraviolet signals arise from the reprocessing of X-ray pulsations in the structures fixed in the binary reference frame. Only harmonics and orbital sidebands of the white dwarf spin frequency are observed, not the spin frequency itself (Patterson and Szkody, 1993).

Fast ultraviolet spectroscopy of YY Dra with coordinated U, B, V, R and I photometry, and Hα spectroscopy found 16% semiamplitude pulses with a period of 264.7(1) s in the UV continuum. There was no evidence for power at twice this period. The UBV pulses were in phase with the UV continuum pulsation. The white dwarf spin period has been refined and is 529.31 ± 0.02 s. Optical pulses at 273(1) s have also been detected. Variations in the C IV line profile were seen over the spin period. Faint, broad line wings extending to $\pm$3000 km/s appear simultaneously with the continuum pulsation maxima (Haswell et al., 1997).

The data of long ROSAT HRI observations show that YY Dra exhibits a double-peaked X-ray pulse profile. It has been argued that the short spin period of the white dwarf in the object indicates that it has a weak magnetic field (Norton et al., 1999).

2.3. GK Persei

GK Persei is an old nova (Nova Persei, 1901) which erupted in 1901 with $V = 0.2$ mag at a maximum, and now the system is at its minimum brightness, $V \approx 13$ mag. Its light curve shows 2–3 mag outbursts which last several months and recur quasiregularly every $n \cdot 400$ days (Subbadin and Bianchini, 1983).

The spectrum of GK Per shows absorption and emission lines varying with an orbital period of $1^d.997$ in anti-phase (Crampton et al., 1986). The X-ray light curve observed during an optical outburst revealed very strong pulsations (modulation depth to maximum flux $\sim$ 50%) with a 351 s pulse period which was attributed to the spin period of the magnetic white

dwarf (Watson et al., 1985).

Two X-ray observations of GK Per in quiescence made with EXOSAT confirmed the 351 s pulse period first discovered during the earlier outburst. A substantial variability of the modulation depth, and possibly the pulse profile, in the observation on timescales of hours was observed (Norton et al., 1988). The 351 s pulse period has also been found in the ultraviolet light curve of GK Per (Patterson, 1991).

Ginga observations of the old nova GK Persei in quiescence, as well as a brief scanning observation during an outburst detected the 351 s spin modulation, which confirms the results of the previous EXOSAT observations (Ishida et al., 1992).

A coherent S–wave modulation with the 351 s spin period in the optical emission lines of GK Per has been found. The pulsed fraction of the Balmer and HeII line fluxes was 4% and 8%, respectively (Reinsch, 1994). The spectrophotometry of GK Per, performed during the 1996 dwarf nova outburst, revealed the white dwarf spin period in line fluxes, V/R ratios, and Doppler-broadened emission profiles (Morales–Rueda et al., 1999).

3. Observations and data reduction

Spectral observations were carried out at the Special Astrophysical Observatory between March 1996 and December 1998 using the spectrograph SP–124 placed at the Nasmyth secondary focus of the 6 m Big Telescope Azimuthal (BTA) (Ioannisiani et al., 1982). The spectrograph equipped with a 1200 lines/mm grating gave a reciprocal dispersion of 50 Å/mm. A multichannel photon-counting system or a television scanner with two lines of 1024 channels recorded two spectra simultaneously (Somova et al., 1982; Drabek et al., 1986; Afanasiev et al., 1991). The observations of GK Per were performed with the analyzer of circular and linear polarization (Najdenov & Panchuk, 1996), which was installed in front of the slit of the spectrograph. A 2–arcsecond slit was used. The spectra were obtained in a wavelength passband of $\approx$ 1000 Å within the range 3900–5100 ÅÅ with a dispersion of 1 Å/channel (spectral resolution $\approx$ 3 Å) and a temporal resolution of 32 ms. The spectra were recorded continuously, and a He–Ne–Ar lamp was observed between the exposures for wavelength calibration. The log of our observations is presented in Table 1.

Power spectra were calculated with the help of a special algorithm. Its mathematical justification is presented in Appendix of the Somov et al. (1998a) paper. The range of periods for analysis varied depending on the object. For BG CMi the period of interest is 913 s, and the range of the investigated periods from 300 s to 2000 s was chosen. The resolution along the period was 5 s in the range from 300 s to 600 s, 10 s in the range 600–1200 s and 50 s in the range 1200–2000 s. For YY Dra and GK Per the periods of interest are 265–275 s, 530 s and 351 s and the range of the investigated periods was from 100 s to 666.6 s, or the scale of periods for BG CMi was divided by a scale factor of 3. To study the oscillations around 530 s in YY Dra, we used a scale factor of 1.5, in this case the period of interest was in the middle of the periodogram. The power, amplitude and phase of the oscillations in relative units (the level of the continuous spectrum is equal to 1) for every channel (wavelength) were calculated.

The relative intensity of emission lines in the spectra of YY Dra is significantly greater than in those of BG CMi and GK Per. It leads to distortion of power spectra in the wavelength ranges corresponding to the emission lines. To compensate this effect we have normalized every section of the power spectra along the period so that the mean values of the sections in the range of periods from 300 to 500 s are equal. We will name such power spectra as normalized ones.

To estimate the time of coherence of the NBOs, an additional temporal resolution for the power spectra was introduced in the current study as we did in the study of V405 Aur (Somov et al., 2000a, b).

The wavelengths were calibrated (Kopylov et al., 1986) with the help of a He–Ne–Ar lamp. To check possible instrumental effects, we observed standard stars. No significant features in the power spectra of the standard stars were found.

4. Results

4.1. BG Canis Minoris

The result of the power spectrum calculation for the exposure 12/27/98–10, see Table 1, is presented in Fig. 1 as a grey–scale image. The level of the grey intensity is proportional to the power of spectral oscillations in arbitrary units. The blackest features in the power spectrum are seen at the periods in the vicinity of the period 913 s corresponding to the spin period of the white dwarf.

The section of the power spectrum along the wavelength corresponding to the 910 s period (bottom) and relative intensity (normalized to the continuum) spectrum (top) illustrate this property in Fig. 2.

The scales of the power and relative intensity in this figure are expressed in arbitrary units, but the zero level for the upper spectrum is shifted and corresponds to 60 units. The wavelengths of the features in the power spectrum are mainly inside the profiles of the Balmer and HeII 4686 Å emission lines. It is easily seen that the power of oscillations is concentrated only in the red or blue wing of the emission lines. The monochromatic power spectrum or the section of the power spectrum over the period correspond-

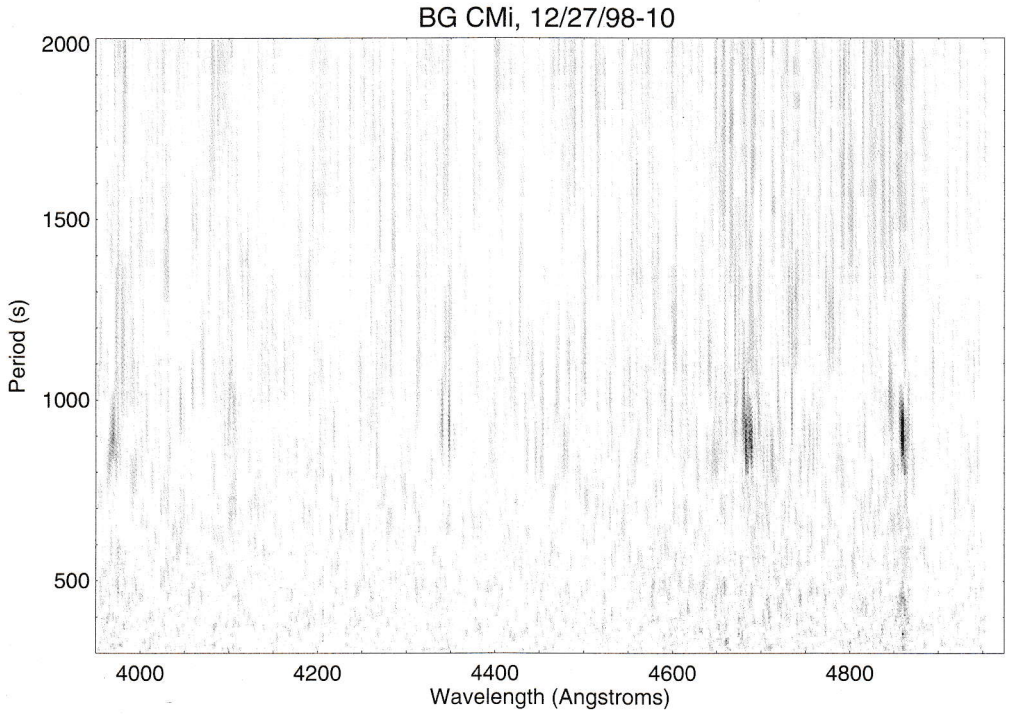

Figure 1: *A grey-scale image of the power spectrum of BG CMi. The level of grey intensity is proportional to the power of spectral oscillations in arbitrary units.*

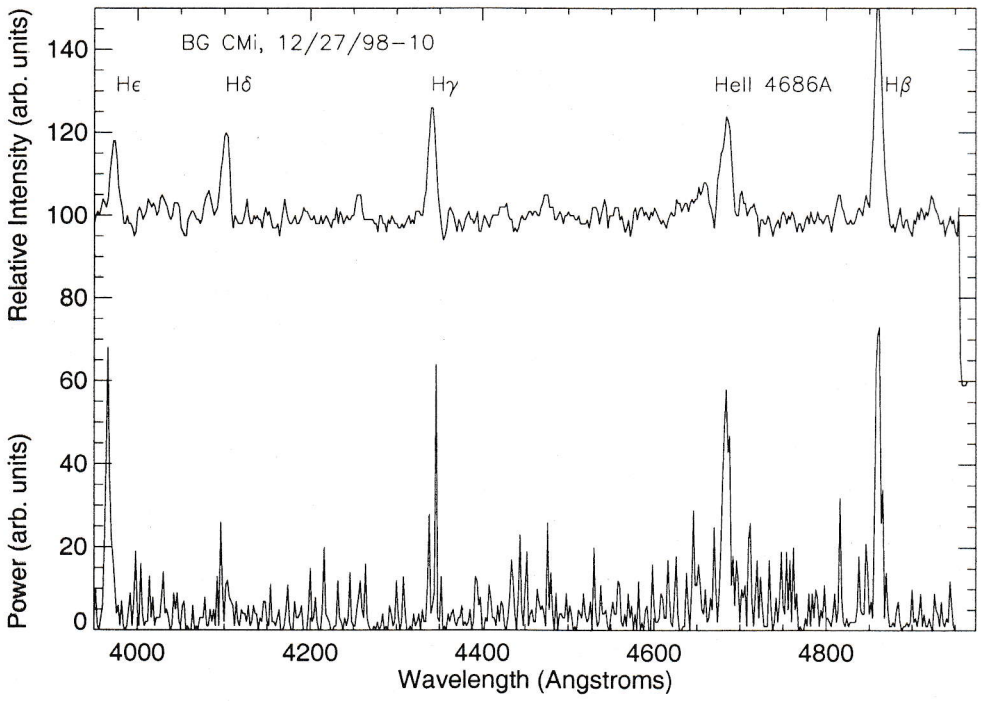

Figure 2: *The section of the power spectrum corresponding to the 910 s spin period of the white dwarf and the relative intensity spectrum (top).*

Table 1: *Journal of the observations*

Object	Date (mm/dd/yy)	Number of the exposure	Start (UT time)	Exposure (s)	Mode
BG CMi	03/17/96	03	17:31:30	5390	spectrum
BG CMi	12/27/98	10	23:02:25	6375	spectrum
YYDra	12/27/98	12	02:18:43	5082	spectrum
YYDra	12/28/98	11	02:06:15	6320	spectrum
GK Per	12/28/98	03	17:41:45	3037	circular polarization
GK Per	12/28/98	06	21:18:00	4042	linear polarization

ing to the wavelength 3966 Å in the profile of the Hϵ emission line is displayed in Fig. 3. The coincidence of the maximum of the strong feature in the monochromatic power spectrum with the 913 s period (upper arrow) is readily seen.

The widths of the features in the power spectrum are also different. Comparison of the widths of the features in Fig. 2 makes evident the presence of relatively wide features (8–10Å), for example, in the Hϵ emission line, and of very narrow (2–3Å), like the one in the Hγ profile. We have already observed similar wide features in the power spectra of PQ Gem (Somov et al., 1998a), and it is interesting to examine them in more detail. The sequence of the monochromatic power spectra in the wavelength range from 3961Å (bottom) to 3970Å (top) with a step of 1Å is shown in Fig. 4. The power spectra were calculated using the whole exposure. In addition, we have computed similar power spectra for the subexposures 0–3000 s, 1000–4000 s and 2000–5000 s, where the first and the second numbers correspond to the times of the beginning and the end of the subexposures within the whole exposure. The results of the calculations for the subexposures 0–3000 s and 2000–5000 s are depicted in Figs. 5 and 6, respectively. It is seen in these figures that the maximum of power in the subexposure 0–3000 s is significantly redshifted relative to the subexposure 2000–5000 s. This means that the broadening of the features cannot be attributed to the spin rotation of the white dwarf, and one should search for an explanation in other physical processes in the system. For comparison the sequence of the monochromatic power spectra in the wavelength range from 4341Å (bottom) to 4350Å (top) with a step of 1Å is shown in Fig. 7. The simultaneous presence of the wide (Fig. 4) and narrow (Fig. 7) features can be explained by the short time of coherence of the oscillations and their transient character. We suppose that the broadening of the features is the result of the orbital rotation of the white dwarf. An analysis of the power spectra of the subexposures yields an estimate of the time of coherence of the monochromatic oscillations of about 3000 s.

The amplitude of the oscillations was up to 50% during the 3000 s subexposures.

The statistical significance or the probability of random origin of the NBOs is estimated at $\sim 10^{-8}$.

4.2. YY Draconis

A grey–scale image of the normalized power spectrum for the exposure 12/27/98–12 is presented in Fig. 8. The level of the grey intensity is proportional to the normalized power of spectral oscillations in arbitrary units. Two statistically significant features in the power spectrum can be seen. The first is located in the Hβ profile at the period of 530 s, corresponding to the white dwarf spin period. The second manifests itself in the Hϵ profile at the period of 265 s, corresponding to the harmonic of the white dwarf spin frequency. The sections of the normalized power spectrum along the wavelength corresponding to the 530 s period (bottom) and to the 265 s period (middle) with the relative intensity spectrum (top) are presented in Fig. 9. The scales of the power and relative intensity in this figure are expressed in arbitrary units, but zeros for the top and middle spectra are shifted and correspond to 60 and 20 units, respectively.

The fragment of the section of the normalized power spectrum along the wavelength corresponding to the 530 s period (bottom) with the relative intensity spectrum (top) are presented in Fig. 10. The scales of the power and relative intensity in this figure are expressed in arbitrary units, but zero for the top spectrum is shifted and corresponds to 60 units. It is readily seen in Fig. 10 that the feature in the power spectrum cannot be attributed to the whole emission line but should be assigned to its segment or component. Such components show themselves up exclusively in the power spectra.

High relative intensity of emission lines in the spectrum leads to a noticeable difference between the power of the noise oscillations in the continuous spectrum and emission lines. This property was compensated by additional normalization which was described above. The estimate of the statistical significance of the features is $10^{-6} - 10^{-8}$.

The amplitude of the oscillations was up to 70% during the 2000 s subexposures. It should be noted that we measured the amplitudes of oscillations rela-

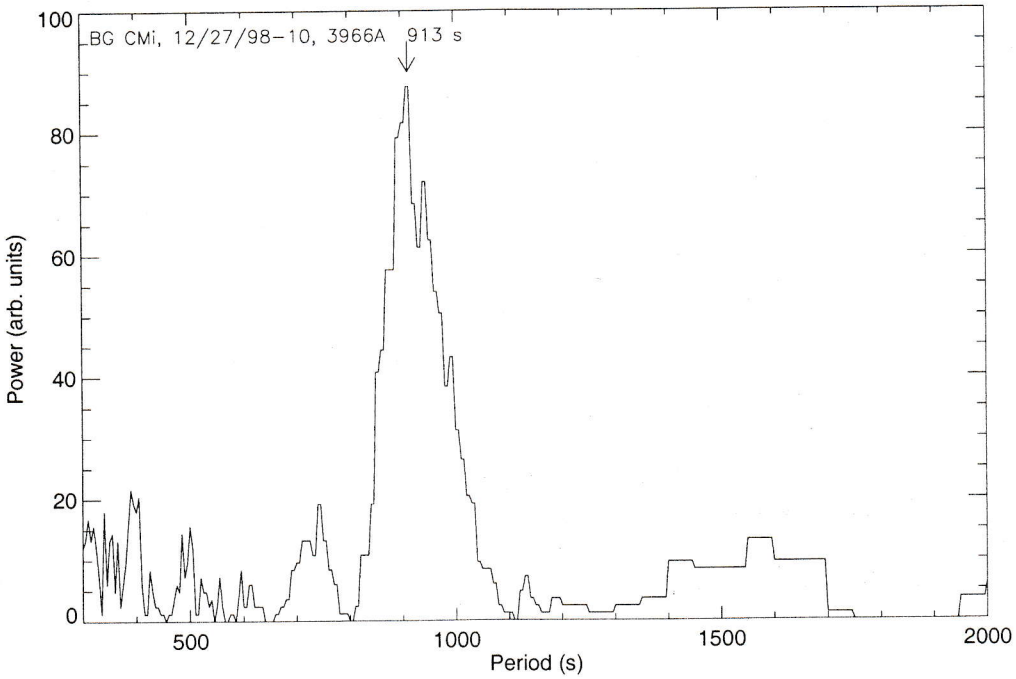

Figure 3: *The section of the power spectrum, presented in Fig. 1, along the period corresponding to the wavelength 3966 Å.*

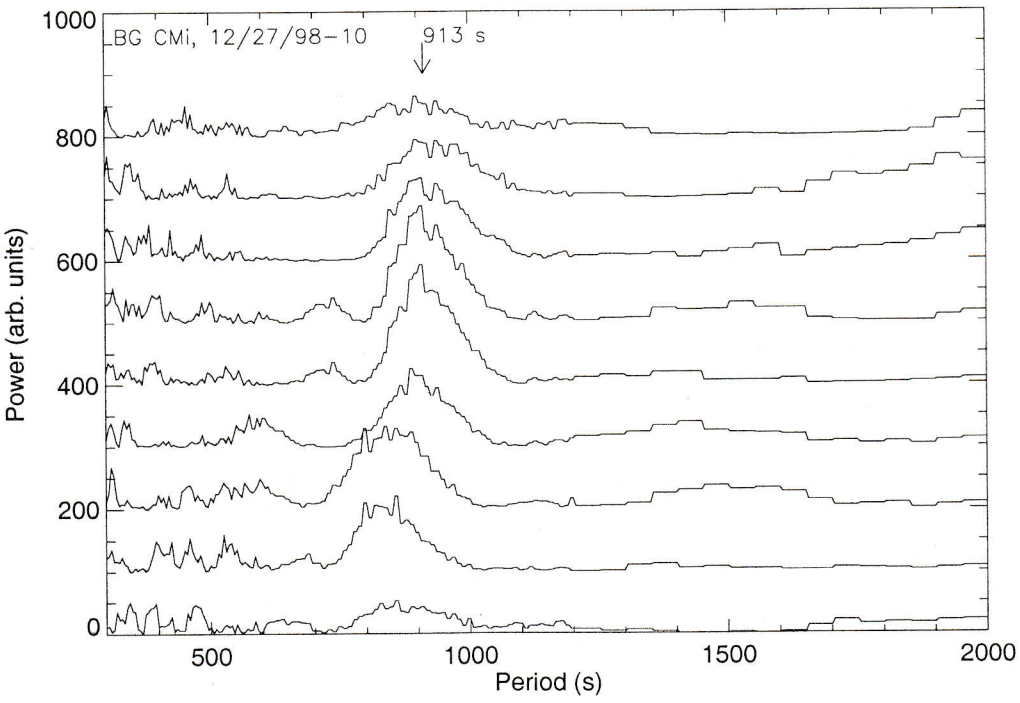

Figure 4: *The sections of the power spectrum along the period corresponding to the wavelengths from 3961 Å (bottom) to 3969 Å (top) with a step of* ≈ 1*Å. The power spectrum was calculated for the whole exposure.*

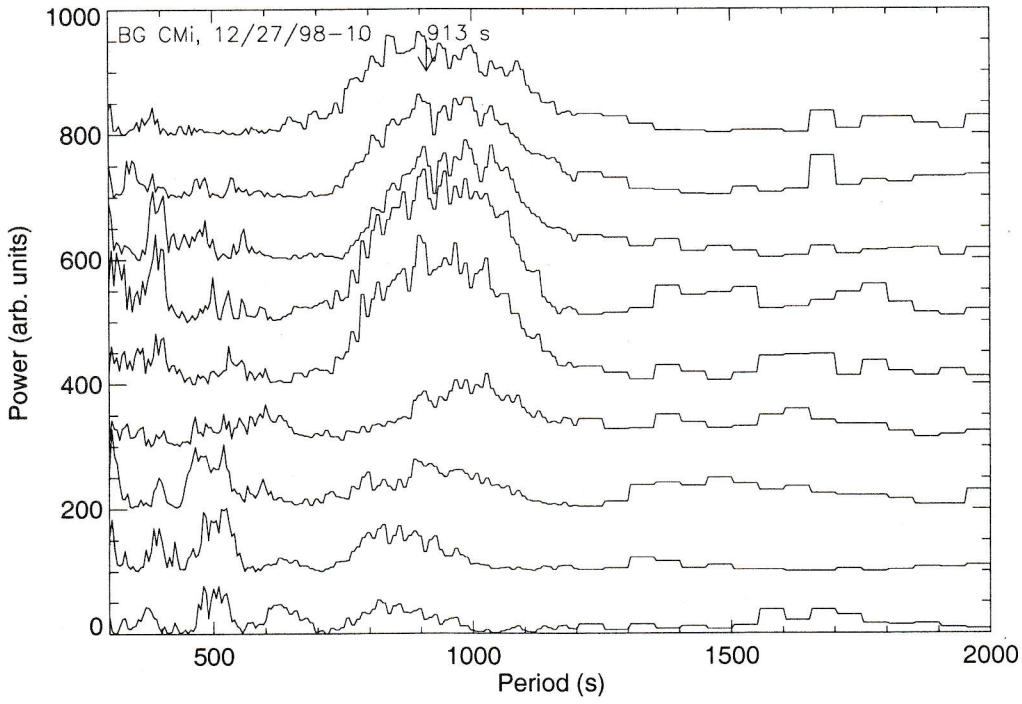

Figure 5: *The sections of the power spectrum along the period corresponding to the wavelengths from 3961 Å (bottom) to 3969 Å (top) with a step of* ≈ 1*Å. The power spectrum was calculated for the subexposure 0–3000 s.*

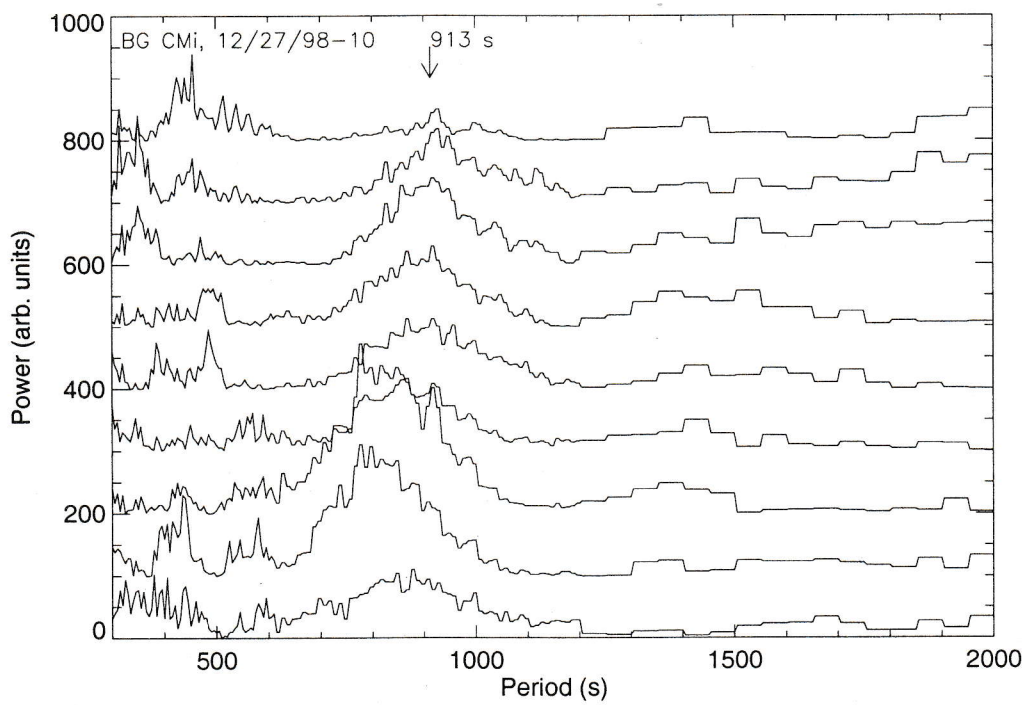

Figure 6: *The sections of the power spectrum along the period corresponding to the wavelengths from 3961 Å (bottom) to 3969 Å (top) with a step of* ≈ 1*Å. The power spectrum was calculated for the subexposure 2000–5000 s.*

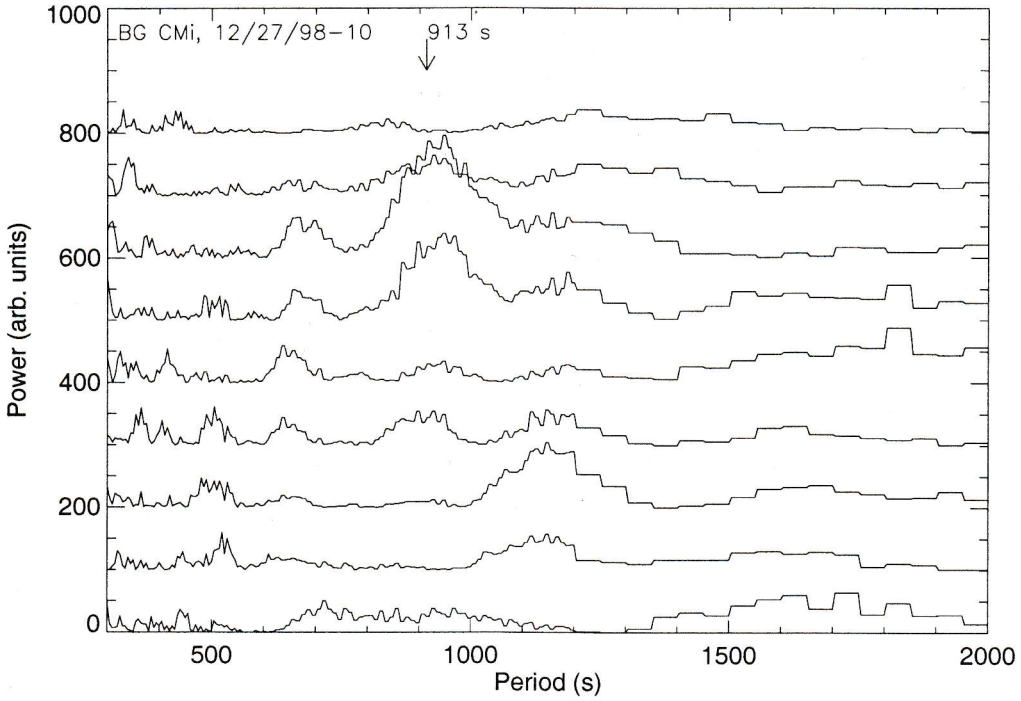

Figure 7: *The sections of the power spectrum along the period corresponding to the wavelengths from 4341 Å (bottom) to 4349 Å (top) with a step of* $\approx$ *1Å. The power spectrum was calculated for the whole exposure.*

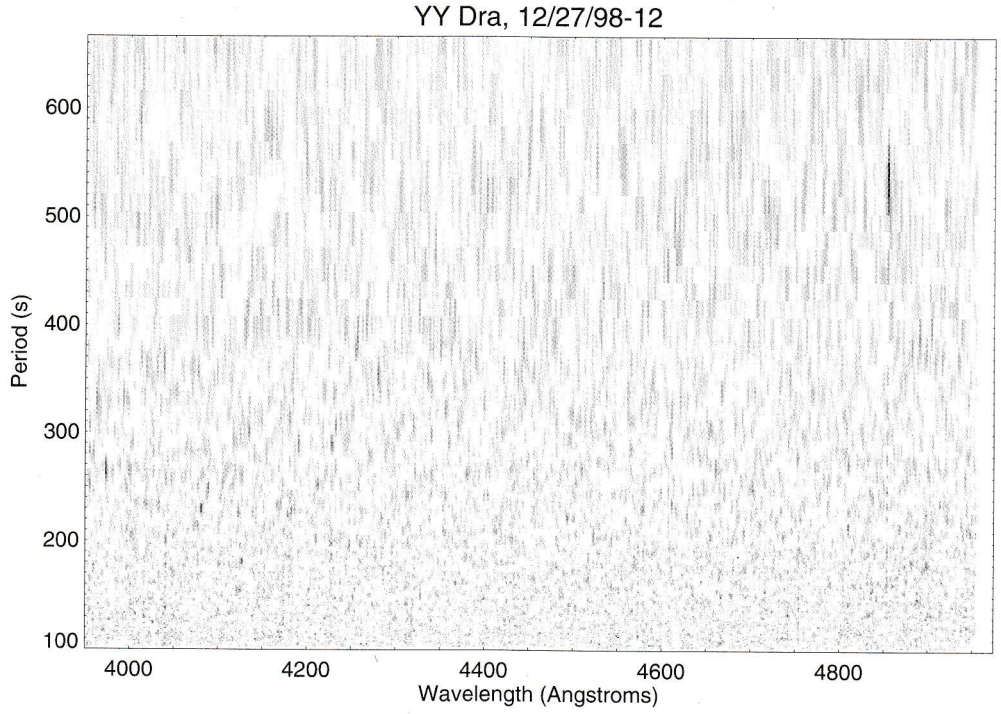

Figure 8: *A grey-scale image of the normalized power spectrum of YY Dra. The level of grey intensity is proportional to the normalized power of spectral oscillations in arbitrary units.*

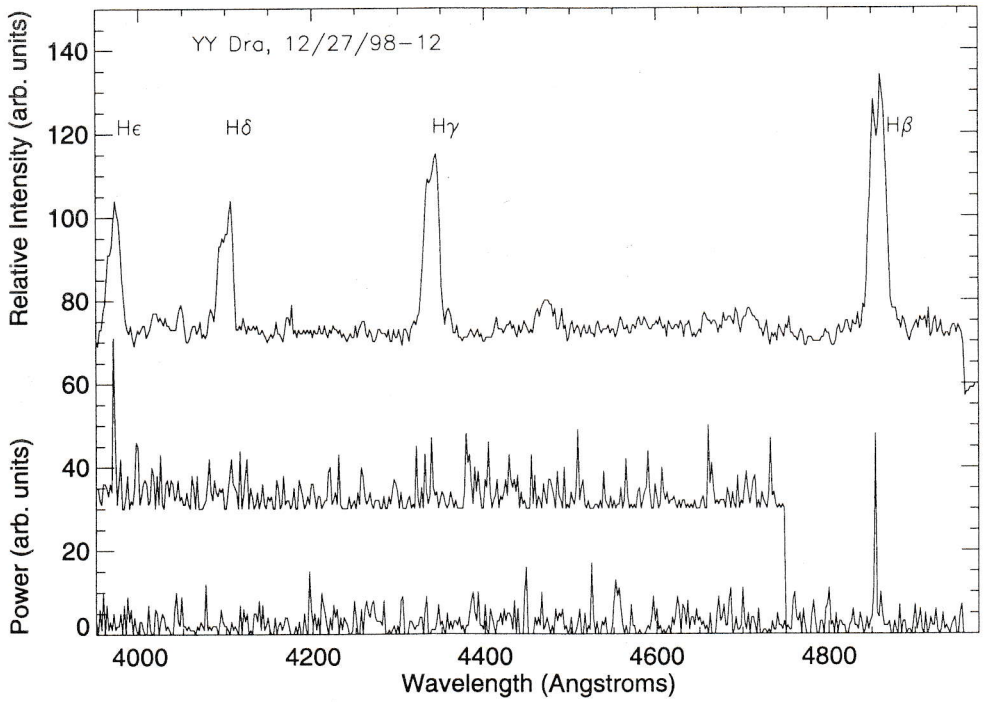

Figure 9: *The sections of the power spectrum corresponding to the 530 s (bottom) and 265 s (middle) periods and the relative intensity spectrum (top).*

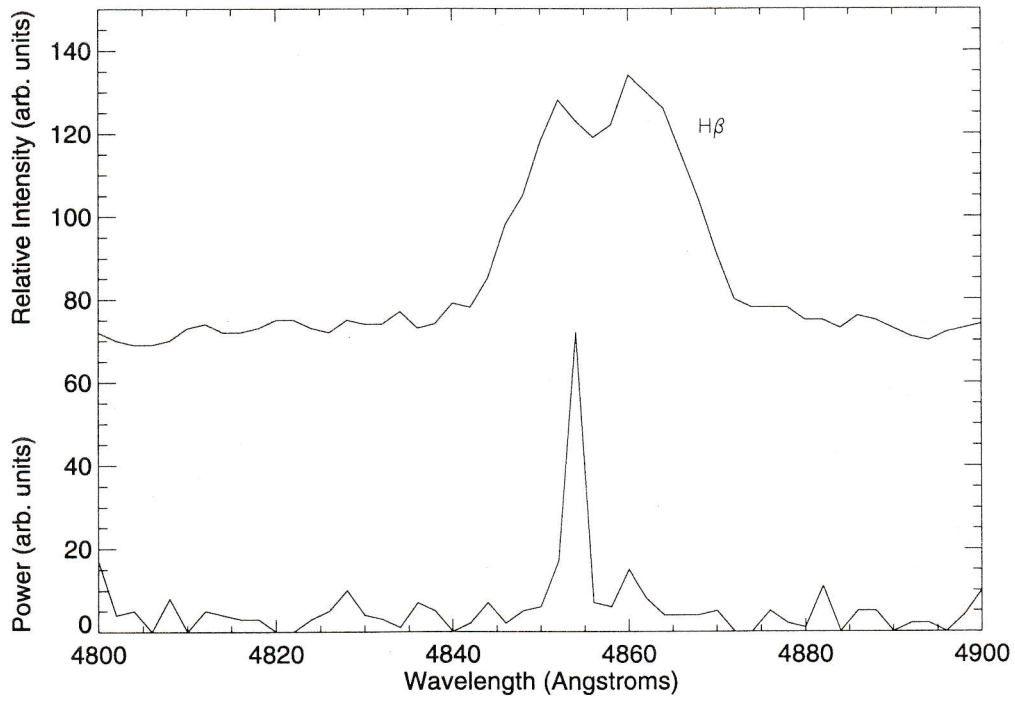

Figure 10: *The fragment of the section of the power spectrum of YY Dra corresponding to the 530 s (bottom) period and the fragment of the relative intensity spectrum (top) in the wavelength range 4800–4900Å.*

tive to the continuous spectrum. The recalculation of the amplitudes relative to the mean intensity noticeably decreases the latter and in the case of YY Dra the 70% amplitude converts to a 16% one.

The monochromatic power spectrum or the section of the power spectrum over the period corresponding to the wavelength 3970 Å in the profile of the Hϵ emission line is shown in Fig. 11. A similar monochromatic power spectrum at the wavelength 4854 Å in the profile of the Hβ emission line is shown in Fig. 12. To see better the coincidence of the maximum of the feature in the spectrum with the 530 s period (upper arrow), we recalculate the power spectrum adjusting the scale of the period so that the spin period is close to the middle in the figure.

The coincidence of the maximum of the strong feature in the monochromatic power spectrum with the 530 s period is readily seen. Using the described-above method of subexposures, we estimated the time of coherence of the NBOs, which is about 3000 s for the oscillations in the profile of the Hβ emission line and about 2000 s for the oscillations in the profile of the Hϵ emission line.

It is important to note that in the second exposure the NBOs were detected only in the profile of the Hδ emission line at the spin period.

4.3. GK Persei

A grey–scale image of the power spectrum for the exposure 12/28/98–3 is presented in Fig. 13. The level of the grey intensity is proportional to the power of spectral oscillations in arbitrary units. No statistically significant features in the power spectrum are seen. The same result was obtained in both exposures in all polarization channels.

5. Discussion

Comparison of the variations over spin periods in emission lines in other observations with our results shows that the presence of the NBOs in emission lines is compatible with the oscillations of the V/R ratio, equivalent width or radial velocity of emission lines over the spin period or its harmonic. The conventional interpretation of these variations or an "accretion curtain" model in which the disk feeds gas to the white dwarf can be found in Patterson (1994), Rosen et al. (1988), Ferrario et al. (1993). The NBOs were detected in the power spectra of PQ Gem (Somov et al., 1997, 1998a, b). On the basis of the observational properties of the NBOs, we have concluded that not only an "accretion curtain" model is insufficient, but their interpretation in the frame of conventional physics is impossible and, as a consequence, we have proposed an advanced hypothesis (Somov et al., 1998a, b). Basing on the additional spectral observations of V405 Aur with the circular and linear polarization analyzers, we suggest, as a development of the hypothesis, that the NBOs can be considered as signatures of elementary particles (Somov et al., 2000a, b).

To compare the NBOs in power spectra of different IPs we have counted formally the number of the events of detection of the NBOs in one exposure and assume the same wavelength range and equal exposures. It has been found that the number of NBO-events in the power spectra of PQ Gem, V405 Aur and BG CMi is greater (4–5 events) than in the power spectra of YY Dra (1–2 events) and GK Per (0 events).

The magnetic field strength of the white dwarf in PQ Gem, V405 Aur and BG CMi is comparable with that of polars (8–18 MG, Piirola et al., 1993; 9–21 MG, Vaeth et al., 1996; Haberl and Motch, 1995; Penning et al., 1986; West et al., 1987). On the other hand, YY Dra and GK Per have a weak magnetic field (Norton et al., 1999). This relationship between the strength of the magnetic field and the number of the NBO-events is an additional argument in favour of the presence of strong magnetic fields (Somov et al., 1998a) in the regions of formation of the radiation causing the NBO-events in the power spectra. However, the number of the NBO-events in the power spectra of PQ Gem and V405 Aur was noticeably variable, and this probable correlation needs an additional observational confirmation.

Some power spectra of PQ Gem showed relatively broad features (8–10Å) (Somov et al., 1998a), and we observed them again in the spectra of BG CMi. An additional investigation made in this paper (Figs. 4–7) shows that the maxima of power in the blue and red parts of the features are noticeably separated in time. This property of the broad features does not permit attributing their broadening to the spin rotation of the white dwarf. We suggest that the orbital motion of the white dwarf is responsible for this effect. However, the broadening of features in power spectra can be considered formally as superposition of two or several NBO-events which are close in time and in optical wavelength.

On the basis of our observations of IPs (PQ Gem, V405 Aur, BG CMi, GK Per and YY Dra), we believe that on a time-scale comparable with the time of coherence one can observe the NBOs in their optical spectra or the NBO-events in the power spectra. On a time-scale greater or much greater than the time of coherence we strongly suggest that only statistical description of the NBO-events is possible. The study of statistics of the NBO-events is one of interesting problems of future observations.

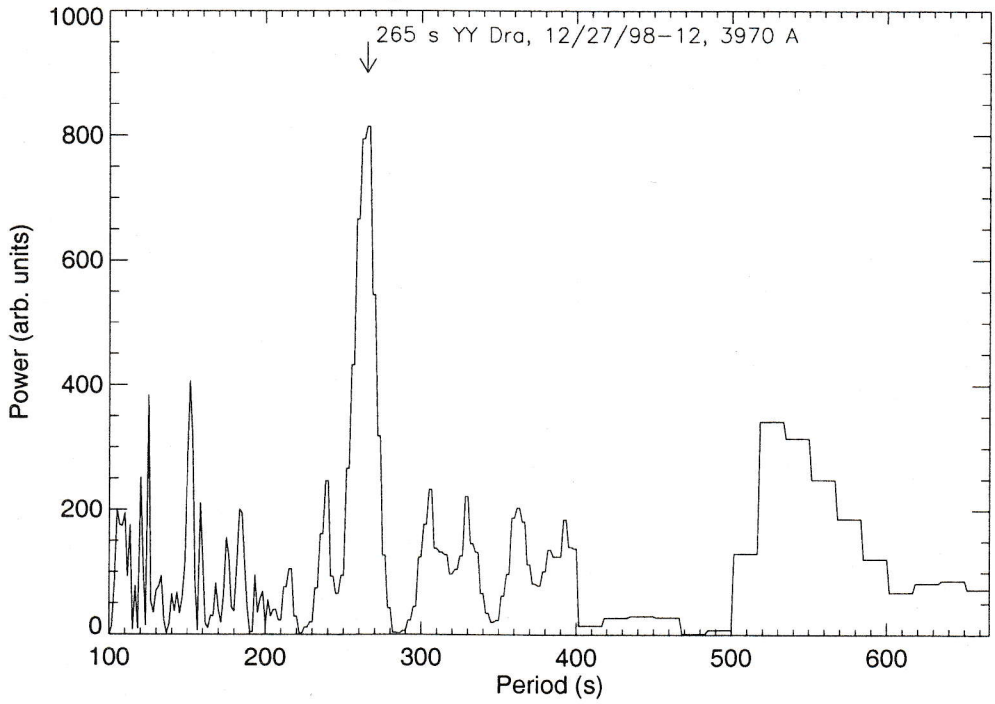

Figure 11: *The section of the power spectrum, presented in Fig. 8, along the period corresponding to the wavelength 3970 Å.*

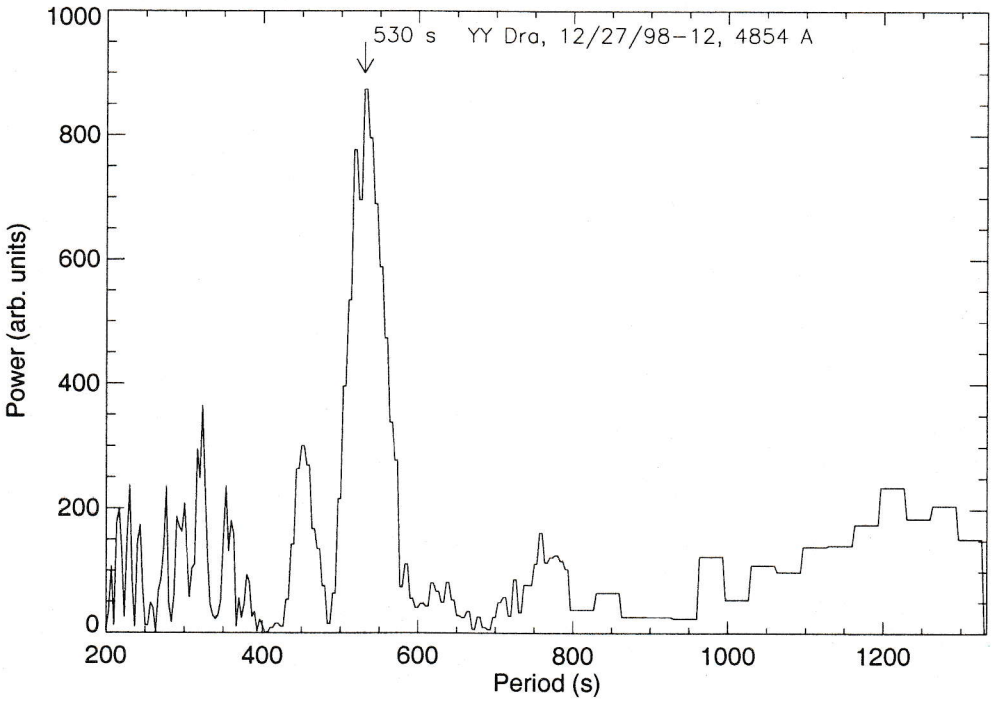

Figure 12: *The section of the power spectrum, presented in Fig. 8, along the period corresponding to the wavelength 4854 Å.*

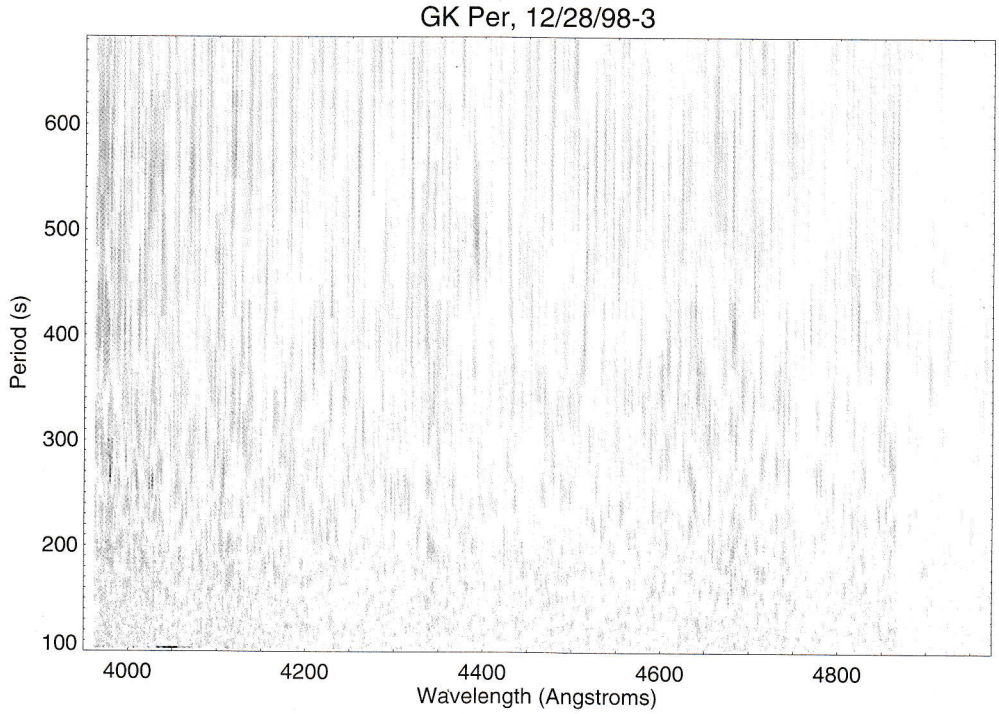

Figure 13: *A grey–scale image of the power spectrum of GK Per which was obtained in the right circular polarization. The level of grey intensity is proportional to the power of spectral oscillations in arbitrary units.*

6. Conclusions

We have presented the results of dynamic spectroscopy of the intermediate polars BG CMi, YY Dra and GK Per obtained at the 6 m telescope with the help of the photon-counting system known as the scanner of BTA. A spectral study of variability of BG CMi and YY Dra revealed narrow–band oscillations (NBOs) or statistically significant features in their power spectra in contrast to GK Per in which the oscillations were not found. The NBOs in the spectra of BG CMi were detected at the spin period of the white dwarf (913 s) in the profiles of Balmer and HeII 4886 Å emission lines. The widths of the features in the power spectra varied from 2–3 Å to 8–10 Å. The power spectra of YY Dra revealed the features at the spin period of the primary and its harmonic. The NBOs in the spectra of GK Per were not found. The formal comparison of the number of the NBO-events in the power spectra shows that this number (4–5 events) is greater in BG CMi than that in the power spectra of YY Dra (1–2 events) and GK Per (0 events). The numbers of the NBO-events in the power spectra of BG CMi, V405 Aur and PQ Gem are about the same, and these objects form a group with polar-like magnetic fields (8–20 MG), while YY Dra and GK Per are attributed to the objects with weak magnetic fields. The relationship between the strength of the magnetic field of the white dwarf and the number of the NBO-events in the power spectra is an additional reason for the presence of strong magnetic fields in the regions of formation of the radiation causing the NBO-events. On the basis of our observations of IPs (PQ Gem, V405 Aur, BG CMi, GK Per and YY Dra), we conclude that on a time-scale much greater than the time of coherence only a statistical description of the NBO-events is possible.

Acknowledgements. This research was supported by the grant of Russian Foundation of Basic Research (RFBR 99–02–18445). We are grateful to I.D. Najdenov for help in the observations of GK Per.

References

Afanasiev V.L., Lipovetsky V.A., Mikhajlov V.P., Nazarov E.A., Shapovalova A.I., 1991, Astrofiz.Issled. Izv. SAO), **31**, 128

Augusteijn T., van Paradijs J., and H.E. Schwarz, 1991, Astron. Astrophys., **247**, 64.

Boroson B., Vrtilek S.D., McCray R., Kallman T., Nagase F., 1996, Astrophys. J., 473, 1079.

Buckley D.,Tuohy I., 1989, Astrophys. J., **344**, 376.

Buckley D.,Tuohy I., 1990, Astrophys. J., **349**, 296.

Crampton D., Fisher W. A., Cowley A. P., 1986, Astrophys. J., **300**, 788.

Cropper M.S., 1990, Space Sci. Rev., **54**, 195

Drabek S.V., Kopylov I.M., Somov N.N., Somova T.A., 1986, Astrofiz.Issled. (Izv. SAO), **22**, 64

Ferrario L., Wickramasinghe D. T., King A. R., 1993, Mon. Not. R. Astron. Soc., **260**, 149

Garlick M. A., Rosen S. R., Mittaz J. P. D., Mason K. O., de Martino D., 1994, Mon. Not. R. Astron. Soc., **267**, 1095

Haberl F., Motch C., 1995, A&A, **297**, L37

Haswell C. A., Patterson J., Thorstensen J. R., Hellier C., Skillman D. R., 1997, Astrophys. J., **476**, 847

Hellier C., Mason K.O., Rosen S.R, Cordova F.A., 1987, Mon. Not. R. Astron. Soc., **228**, 463

Hellier C., Mason K.O., Cropper M.S., 1990, Mon. Not. R. Astron. Soc., **242**, 250

Hellier C., Cropper M.S., Mason K.O., 1991, Mon. Not. R. Astron. Soc., **248**, 233

Ioannisiani B.K., Neplokhov E.M., Kopylov I.M., Rylov V.S. & Snezhko L.I. , 1982, in: Instrumentation for Astronomy with Large Optical Telescopes, ed. C.M. Humphries, Reidel, 3

Ishida M., Sakao T., Makishima K., Ohashi T., Watson M. G., Norton A. J., Kawada M., Koyama, K., 1992, Mon. Not. R. Astron. Soc., **254**, 647

Kopylov I.M., Somov N.N., Somova T.A., 1986, Astrofiz.Issled. (Izv. SAO), **22**, 77

Mateo M., Szkody P., Garnavich P., 1991, Astrophys. J., **370**, 370

de Martino D., Mouchet M., Bonnet-Bidaud J. M., Vio R., Rosen S. R., Mukai K., Augusteijn T., Garlick M. A., 1995, Astron. Astrophys., **298**, 849

McHardy I.M., Pye J.P., Fairall A. P., Warner B., Allen S., and Cropper M., 1984, Mon. Not. R. Astron. Soc., **210**, 663

McHardy I.M., Pye J.P., Fairall A. P., and Menzies J.W., 1987, Mon. Not. R. Astron. Soc., **225**, 355

Morales-Rueda L., Still M. D., Roche P., 1999, Mon. Not. R. Astron. Soc., **306**, 753

Najdenov I.D., Panchuk V.E., 1996, Bull. Spec. Astrophys. Obs., **41**, 145

Norton A. J., Watson M. G., King A. R., 1988, Mon. Not. R. Astron. Soc., **231**, 783

Norton A.J., McHardy I.M., Lehto H.J., and Watson M.G., 1992, Mon. Not. R. Astron. Soc., **258**, 697

Norton A. J., Beardmore A. P., Allan A., Hellier C., 1999, Astron. Astrophys., **347**, 203

Patterson J., 1991, Publ. Astr. Soc. Pacific, **103**, 1149

Patterson J., Schwartz D. A., Pye J. P., Blair W. P., Williams G. A., Caillault J. P., 1992, Astrophys. J., **392**, 233

Patterson J., Thomas G., 1993, Publ. Astr. Soc. Pacific, **105**, 59

Patterson J., Szkody P., 1993, Publ. Astr. Soc. Pacific, **105**, 1116

Patterson J., 1994, Publ. Astr. Soc. Pacific, **106**, 209

Penning W.R., 1985, Astrophys. J., **289**, 300

Penning W.R., Schmidt G.D., and Liebert J., 1986, Astrophys. J., **301**, 881

Piirolla V., Hakala P., Coyne G.V., 1993, Astrophys. J., **410**, L107

Reinsch K., 1994, Astron. Astrophys., **281**, 108

Rosen S. R., Mason K. O., Cordova F. A., 1988, Mon. Not. R. Astron. Soc., **231**, 549

Somova T.A., Somov N.N., Markelov S.V., Nebelitsky V.B., Spiridonova O.I., Fomenko A.F., 1982, in: Instrumentation for Astronomy with Large Optical Telescopes, ed. C.M. Humphries, Reidel, 283

Somov N.N., Somova T.A., Najdenov I.D., 1997, in: Stellar magnetic fields, Proceedings of the International Conference (Nizhnij Arkhyz, 13–18 May 1996), eds.: Glagolevskij Yu.V., Romanyuk I.I., Moscow, 141

Somov N.N., Somova T.A., Najdenov I.D., 1998a, Astron. Astrophys., **332**, 526

Somov N.N., Somova T.A., Najdenov I.D., 1998b, Astron. Astrophys., **335**, 583

Somov N.N., Somova T.A., Najdenov I.D., 2000a, in: Magnetic fields of chemically peculiar and related stars, Proceedings of the International Conference (Nizhnij Arkhyz, 24–27 September 1999) eds.: Glagolevskij Yu.V., Romanyuk I.I., Moscow, 229

Somov N.N., Somova T.A., Najdenov I.D., 2000b, Bull. Spec. Astrophys. Obs., **50**, 80

Subbadin F., Bianchini A., 1983, Astron. Astrophys. Suppl. Ser., **54**, 393

Vaeth H., Chanmugam G., Frank J., 1996, Astrophys. J., **457**, 407

Watson M.G., King A.R., Osborne J., 1985, Mon. Not. R. Astron. Soc., **212**, 917

West S.C., Berriman G., and Schmidt G.D., 1987, Astrophys. J., **322**, L35